NATIONAL ADVISORY COMMITTEE FOR AERONAUTICS

REPORT No. 720

PRESSURE AVAILABLE FOR COOLING WITH COWLING FLAPS

By GEORGE W. STICKLE, IRVEN NAIMAN, and JOHN L. CRIGLER

1941

AERONAUTIC SYMBOLS

1. FUNDAMENTAL AND DERIVED UNITS

	Symbol	Metric		English	
		Unit	Abbreviation	Unit	Abbreviation
Length	l	meter	m	foot (or mile)	ft (or mi)
Time	t	second	s	second (or hour)	sec (or hr)
Force	F	weight of 1 kilogram	kg	weight of 1 pound	lb
Power	P	horsepower (metric)		horsepower	hp
Speed	V	kilometers per hour	kph	miles per hour	mph
		meters per second	mps	feet per second	fps

2. GENERAL SYMBOLS

W Weight $=mg$

g Standard acceleration of gravity $=9.80665$ m/s^2 or 32.1740 ft/sec^2

m Mass $=\frac{W}{g}$

I Moment of inertia $=mk^2$. (Indicate axis of radius of gyration k by proper subscript.)

μ Coefficient of viscosity

ν Kinematic viscosity

ρ Density (mass per unit volume)

Standard density of dry air, 0.12497 kg-m^{-4}-s^2 at 15° C and 760 mm; or 0.002378 lb-ft^{-4} sec^2

Specific weight of "standard" air, 1.2255 kg/m^3 or 0.07651 lb/cu ft

3. AERODYNAMIC SYMBOLS

S Area

S_w Area of wing

G Gap

b Span

c Chord

A Aspect ratio, $\frac{b^2}{S}$

V True air speed

q Dynamic pressure, $\frac{1}{2}\rho V^2$

L Lift, absolute coefficient $C_L=\frac{L}{qS}$

D Drag, absolute coefficient $C_D=\frac{D}{qS}$

D_0 Profile drag, absolute coefficient $C_{D_0}=\frac{D_0}{qS}$

D_i Induced drag, absolute coefficient $C_{D_i}=\frac{D_i}{qS}$

D_p Parasite drag, absolute coefficient $C_{D_p}=\frac{D_p}{qS}$

C Cross-wind force, absolute coefficient $C_C=\frac{C}{qS}$

i_w Angle of setting of wings (relative to thrust line)

i_t Angle of stabilizer setting (relative to thrust line)

Q Resultant moment

Ω Resultant angular velocity

R Reynolds number, $\rho\frac{Vl}{\mu}$ where l is a linear dimension (e.g., for an airfoil of 1.0 ft chord, 100 mph, standard pressure at 15° C, the corresponding Reynolds number is 935,400; or for an airfoil of 1.0 m chord, 100 mps, the corresponding Reynolds number is 6,865,000)

α Angle of attack

ϵ Angle of downwash

α_0 Angle of attack, infinite aspect ratio

α_i Angle of attack, induced

α_a Angle of attack, absolute (measured from zero-lift position)

γ Flight-path angle

REPORT No. 720

PRESSURE AVAILABLE FOR COOLING WITH COWLING FLAPS

By GEORGE W. STICKLE, IRVEN NAIMAN, and JOHN L. CRIGLER
Langley Memorial Aeronautical Laboratory

NATIONAL ADVISORY COMMITTEE FOR AERONAUTICS

HEADQUARTERS, NAVY BUILDING, WASHINGTON, D. C.

Created by act of Congress approved March 3, 1915, for the supervision and direction of the scientific study of the problems of flight (U. S. Code, Title 50, Sec. 151). Its membership was increased to 15 by act approved March 2, 1929. The members are appointed by the President, and serve as such without compensation.

TECHNICAL COMMITTEES

AERODYNAMICS
POWER PLANTS FOR AIRCRAFT
AIRCRAFT MATERIALS

AIRCRAFT STRUCTURES
AIRCRAFT ACCIDENTS
INVENTIONS AND DESIGNS

Coordination of Research Needs of Military and Civil Aviation

Preparation of Research Programs

Allocation of Problems

Prevention of Duplication

Consideration of Inventions

LANGLEY MEMORIAL AERONAUTICAL LABORATORY

LANGLEY FIELD, VA.

AMES AERONAUTICAL LABORATORY

MOFFETT FIELD, CALIF.

Conduct, under unified control, for all agencies, of scientific research on the fundamental problems of flight.

OFFICE OF AERONAUTICAL INTELLIGENCE

WASHINGTON, D. C.

Collection, classification, compilation, and dissemination of scientific and technical information on aeronautics

9-20-41

REPORT No. 720

PRESSURE AVAILABLE FOR COOLING WITH COWLING FLAPS

By George W. Stickle, Irven Naiman, and John L. Crigler

SUMMARY

A full-scale investigation has been conducted in the NACA 20-foot tunnel to determine the pressure difference available for cooling with cowling flaps. The flaps were applied to an exit slot of smooth contour at 0° flap angle. Flap angles of 0°, 15°, and 30° were tested. Two propellers were used; propeller C has conventional round blade shanks and propeller F has airfoil sections extending closer to the hub.

The pressure available for cooling is shown to be a direct function of the thrust disk-loading coefficient of the propeller. The maximum suction obtained with a cowling flap set at 30°, located in a region where the static pressure for the 0° flap position is equal to that of the free air stream, is shown to be equal to approximately one-half the average total pressure of the air stream; the total pressure is given by the sum of the dynamic pressure and the thrust loading. The total pressure in front of the cowling is critically dependent on the ratio of the front opening to the propeller diameter for propeller C. Propeller F gave a higher total pressure in front of the cowling.

For the take-off condiiion, it was found that (1) with the 0° flap, propeller C produced only one-half as much available cooling pressure as propeller F; (2) with the 30° flap, propeller C produced an available cooling pressure three times as large as was obtained with the 0° flap and propeller F produced a pressure difference twice that obtained with the 0° flap; and (3) with the 30° flap and a conductance of 0.118, the pressure drop across the baffle plate with propeller C was 3.17 and with propeller F was 4.85 times the dynamic pressure of the air stream.

INTRODUCTION

The NACA in 1935 conducted an extensive cowling investigation (references 1, 2, and 3) to furnish information in regard to the cowling and cooling of airplane engines under all operating conditions. The investigation showed the effect of different nose forms, skirts, flaps, spinners, and propellers on the efficiency of the engine-cowling combinations and on the available pressure difference for cooling the engine. The chief emphasis in this investigation was on the fitting of all the variables into a rational analysis of the cowling and cooling problem. A smooth contour line for the skirt design was found to be a primary requirement. The earlier tests on cowling flaps were confined to a single series of a design typical of those in use on airplanes at that time. The present report is an extension of the investigation of cowling flaps in which the flap has been applied to a smooth-contour exit-slot design. The results include tests with two full-scale, three-blade, adjustable propellers. One propeller has conventional round blade shanks and the other propeller has the airfoil sections extending closer to the propeller hub.

SYMBOLS

A_2 area of exit slot
D diameter of propeller; drag
ΔD increase of drag when air flows through cowling
C_D estimated drag coefficient (D/qF)
ΔC_D increase in drag coefficient due to passage of cooling air $(\Delta D/qF)$
C_T thrust coefficient $(T/\rho n^2 D^4)$
F projected frontal area of nacelle
H_T total pressure behind propeller
H increase in total pressure produced by propeller
K conductance of engine or baffle plate
K_2 conductance of exit slot (A_2/F)
P power input to propeller
P_c power disk-loading coefficient (P/qSV)
p static pressure on surface of cowling referred to static pressure of free air stream
p_0 static pressure of free air stream
p_f pressure in front of engine or baffle
p_r pressure in rear of engine or baffle
Δp pressure drop across engine or baffle plate $(p_f - p_r)$
ΔP pressure difference available for pumping air
q dynamic pressure of air stream $(\frac{1}{2}\rho V^2)$
Q volume of air flowing through cowling per second
R net force on thrust balance of propeller-nacelle unit
S disk area of propeller
T thrust of propeller $(R+D)$
T_c thrust disk-loading coefficient (T/qS)
V velocity of air stream
x fractional radius of propeller
β blade-angle setting of propeller at 0.75 radius
η propulsive efficiency of propeller (T_c/P_c)
η_n net efficiency of propeller-nacelle unit (RV/P)
η_0 net efficiency of propeller-nacelle unit with no air flow through cowling and exit closed
η_p pump efficiency of cowling
ρ mass density of air

ANALYSIS OF THE PROBLEM

The pumping action of the cowling is dependent on the pressure difference between the entrance and the exit of the cowling. For the condition of high-speed flight, the forward velocity of the airplane produces most of this pressure difference; the cooling problem is therefore usually easy and interest is centered largely

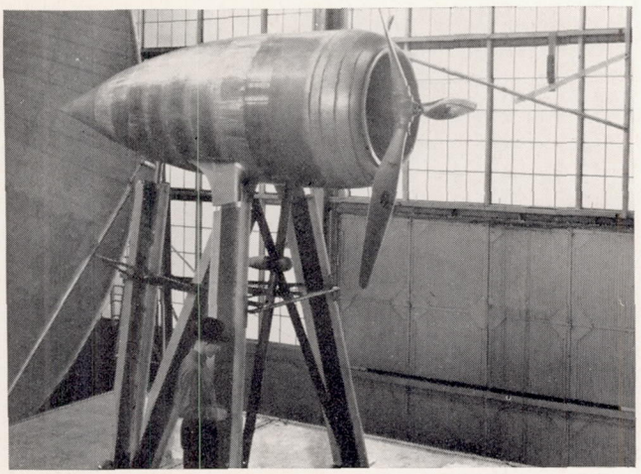

FIGURE 1.—Test set-up in tunnel. (Nose slot was closed for these tests.)

on the efficiency of the cooling. For the static-thrust condition, the propeller produces all the pressure difference. The most difficult cooling conditions are in take-off and climb. As an aid to the analysis of the cooling problem under these conditions, it is desirable to consider the pressures produced by the propeller and the forward velocity.

If the distribution of the thrust is assumed to be uniform over the propeller disk area S and the rotation of the slipstream is neglected, the total pressure in the air stream behind the propeller is

$$H_T=p_0+q+\frac{T}{S}$$

where p_0 and q are measured in the undisturbed air. The increase in total pressure due to the propeller is given by

$$H=\frac{T}{S}$$

If both sides are divided by q,

$$\frac{H}{q}=\frac{T}{qS}=T_c=\eta P_c$$

For a constant value of P_c, changes in thrust distribution and η with blade-angle setting being neglected, the average value of H/q gives the pressure produced by the propeller in terms of the dynamic pressure of the air stream. Because the pumping action of the cowling is dependent on the pressures and the velocities in the propeller slipstream, the pressure increase for the different conditions of propeller operation must be known.

A few feet behind the propeller, the pressure increase has been almost completely converted into velocity. The static pressure in the region of the cowling exit is then almost equal to that of the free air stream. If a flap is extended into the slipstream, the resultant increase of velocity will cause a drop in the static pressure at the exit. A suction at the exit will thereby be produced.

The pressure at the cowling entrance is approximately the dynamic pressure of the air stream, being more or less than this value depending upon the shape of the inner sections of the propeller. The over-all pressure difference ΔP is then the difference between the entrance and the exit pressures. It is thus evident that, by proper design of the inner section of the propeller and of the cowling exit, for the take-off and the climb conditions, over-all pressure differences several times the dynamic pressure of the air stream are obtainable.

The flow equation of the air through the cowling, given in reference 1, may be put in the following form:

$$\Delta P/\Delta p=1+(K/K_2)^2 \qquad (1)$$

This equation specifies the ratio of engine to exit conductance necessary to secure the desired cooling-pressure drop Δp when ΔP is available as over-all pressure difference.

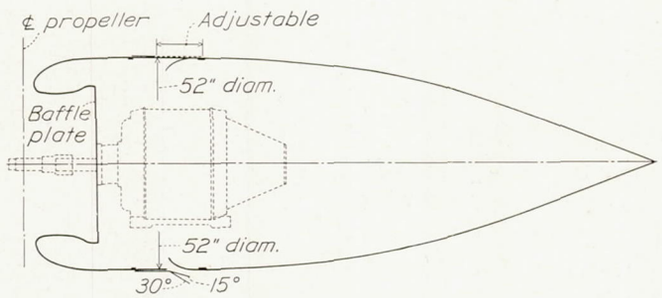

FIGURE 2.—Line drawing of the test arrangements.

In reference 1, the pump efficiency of a cowling was defined as the ratio of the useful cooling power to the increased power required to propel the airplane,

$$\eta_p=\frac{Q\Delta p}{V\Delta D}$$

Alternately, this pump efficiency may be expressed in terms of the net efficiency of the propeller, the engine conductance, and the power disk-loading coefficient as

$$\eta_p=\frac{KF}{SP_c}\ \frac{(\Delta p/q)^{3/2}}{\eta_0-\eta_n}$$

APPARATUS AND TESTS

The investigation was conducted in the NACA 20-foot wind tunnel, which with its standard equipment is described in reference 4. The test set-up was the same as that used in reference 5. Figure 1 shows the general arrangement of the set-up on the tunnel balance. The nose slot was closed for these tests. The skirt was opened at the point shown in the line drawing of the test arrangements (fig. 2). The skirt for the 0° flap

was made of a circular cylinder that could be moved axially to vary the exit area in order to cover the range of cooling pressures for all conditions of flight. The 15° and the 30° flaps were made of conical pieces of metal with 6-inch chords. These flaps were tested in only one position. The nacelle diameter was 52 inches.

A baffle plate, constructed as a shutter with four stops and controlled from the balance house, simulated engine conductances of 0, 0.039, 0.079, and 0.118. The propeller was driven by a 150-horsepower, three-phase,

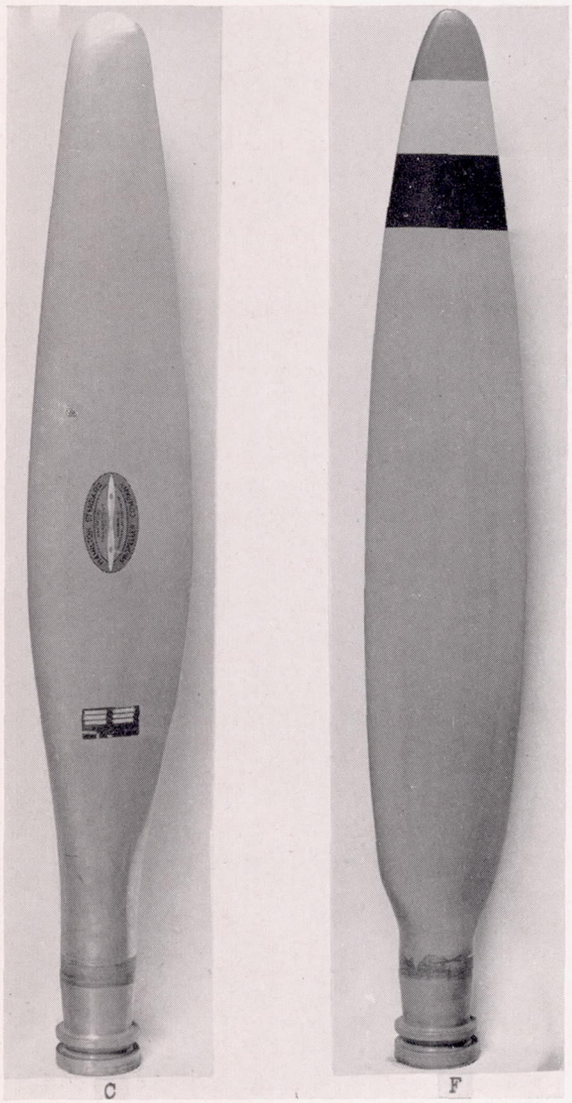

FIGURE 3.—Blades of propellers used.

wound-rotor induction motor mounted in the nacelle. The speed and the power output of the motor were controlled by resistance in the rotor circuit. Pressures inside and outside the exit slot and across the engine baffle were photographically recorded on a multiple-tube manometer.

The propellers used for this investigation are shown in figure 3. Propeller C, with conventional round blade shanks, is Bureau of Aeronautics drawing No. 5868–9; propeller F, with airfoil sections extending closer to the hub, is Bureau of Aeronautics drawing No. 4893. Both propellers are three-blade, adjustable propellers of 10-foot diameter. Details of these propeller blades are given in reference 5. All tests were made with a blade-angle setting of 20° at 0.75 radius.

RESULTS

Table I presents a summary of the results obtained with both propellers. The table is divided into four sections representing conductances of 0, 0.039, 0.079, and 0.118. Each section is further divided into columns for values of $1/\sqrt[3]{P_c}$ of 0.5, 0.6, 1.0, and 1.6. Each of these columns gives the pressure drop across the baffle Δp and the rear pressure p_r as fractions of the dynamic pressure q; each column also gives the net efficiency. The pump efficiency is given in the high-speed condition, $1/\sqrt[3]{P_c}=1.6$, for the 0° flap and is given in the climb condition, $1/\sqrt[3]{P_c}=1.0$, for the 15° and the 30° flaps. The pump efficiency is omitted for the other slot openings and operating conditions because the experimental accuracy did not justify such computations.

The drag coefficient with the propeller removed is given in the last column. The drag values for open exit slots were obtained in the following manner: The basic drag values for the cowling with exit slot closed at zero conductance were obtained by separate drag tests. The basic drag was deducted from the drag of the same cowling-propeller combination at zero power to give the drag of the free-wheeling propeller. The drag of the free-wheeling propeller was then deducted from the drag of the open-exit cowling-propeller combinations at zero power to obtain the values given in table I.

Figures 4, 5, and 6 give the pressure distributions for the 0°, the 15°, and the 30° flaps, respectively, showing the effect of two values of engine conductance and of propeller operating conditions.

The pressure drop for zero conductance is taken as the available pressure difference ΔP. The value of this available pressure difference as a fraction of the dynamic pressure of the air stream is given in figure 7 as a function of the flap angle for several disk loadings.

Figure 8 gives a graphical solution of the flow equation of the air through the cowling (equation (1)). The experimental points for the 0° flap and the high-speed condition of $1/\sqrt[3]{P_c}=1.6$ are plotted on the graph, where $K_2=A_2/F$, for comparison with the theoretical curve. Figure 9 presents similar results for the tests of the 15° and the 30° flaps for the take-off condition, $1/\sqrt[3]{P_c}=0.5$ and 0.6.

A comparison of the cooling-drag coefficient with the pressure drop in the cruising condition is given in figure 10. The drag increase due to cooling was computed from

$$\Delta C_D=(\eta_0-\eta_n)P_c\frac{S}{F}$$

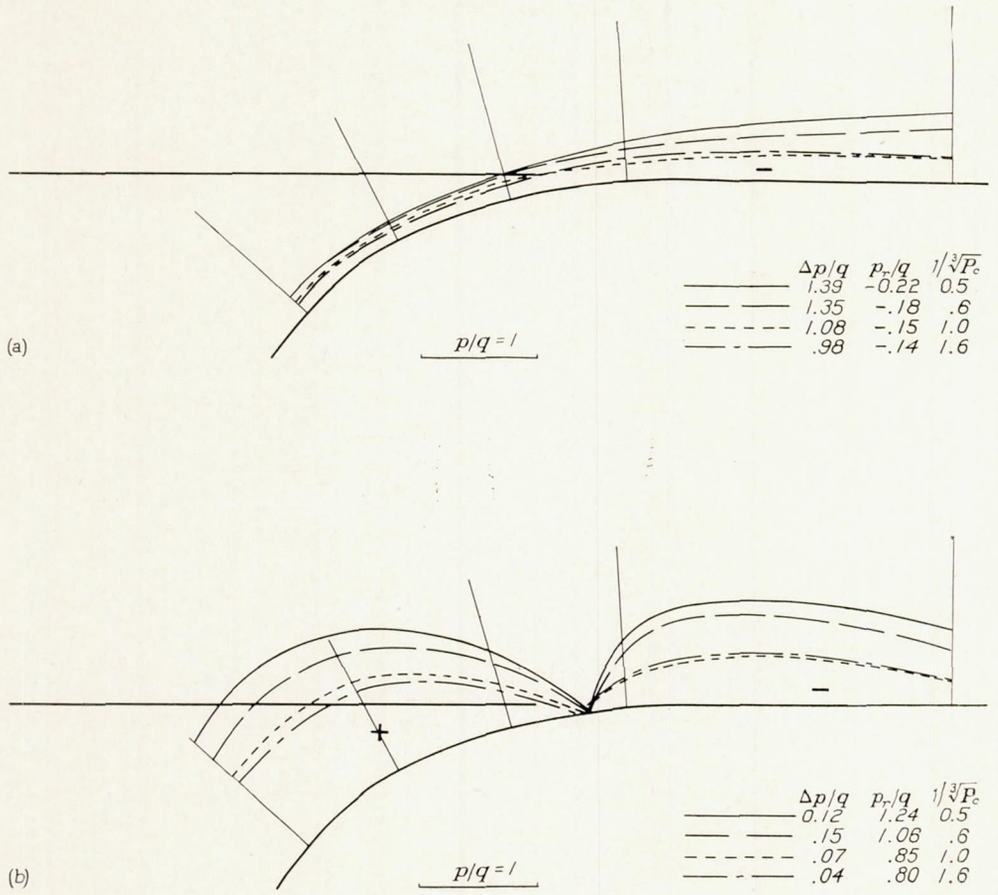

(a) $K=0$.
(b) $K=0.118$.

FIGURE 4.—Pressure distribution for the 0° flap. Opening, ½ inch; propeller C.

At $1/\sqrt[3]{P_c}=1.6$ for a 10-foot propeller on a 52-inch nacelle, this equation becomes

$$\Delta C_D=1.305(\eta_0-\eta_n)$$

From the definition for pump efficiency,

$$\Delta C_D=\frac{K\left(\frac{\Delta p}{q}\right)^{3/2}}{\eta_p}$$

The curve for 100-percent pump efficiency is included for comparative purposes. The section below the base line in the figure indicates the additional form drag for the open nose over the closed streamline nose, as given by unpublished data.

Figure 11 shows the distribution of total-pressure increase behind propeller C, which has round blade shanks, for the different conditions of propeller operation. Figure 12 shows the streamlines around the front of the cowling for high and low slipstream contractions, which correspond to the take-off condition and to the high-speed condition, respectively. Figures 11 and 12 were plotted from unpublished test data.

EFFECT OF FRONT OPENING ON THE AVAILABLE PRESSURE

A study of figure 11 shows that the increase in total pressure behind propeller C varies considerably with propeller operating condition and propeller radius. A blocking effect occurs over the inner two-tenths of the propeller radius but, outside this radius, the total pressure increases rapidly with radius, about 80 percent of the maximum value realized being obtained at $x=0.3$. Inasmuch as the maximum diameter of the front opening of the test arrangement, $x=0.29$, is located in the region of this steep pressure gradient, the pressure obtained from the propeller slipstream is very critical to small changes in the front opening. If more cooling at low airspeed is the determining consideration, it is advantageous to block off the hub and the inner portions of the propeller with a spinner and to increase the diameter of the cowling opening in order to utilize the available front pressure.

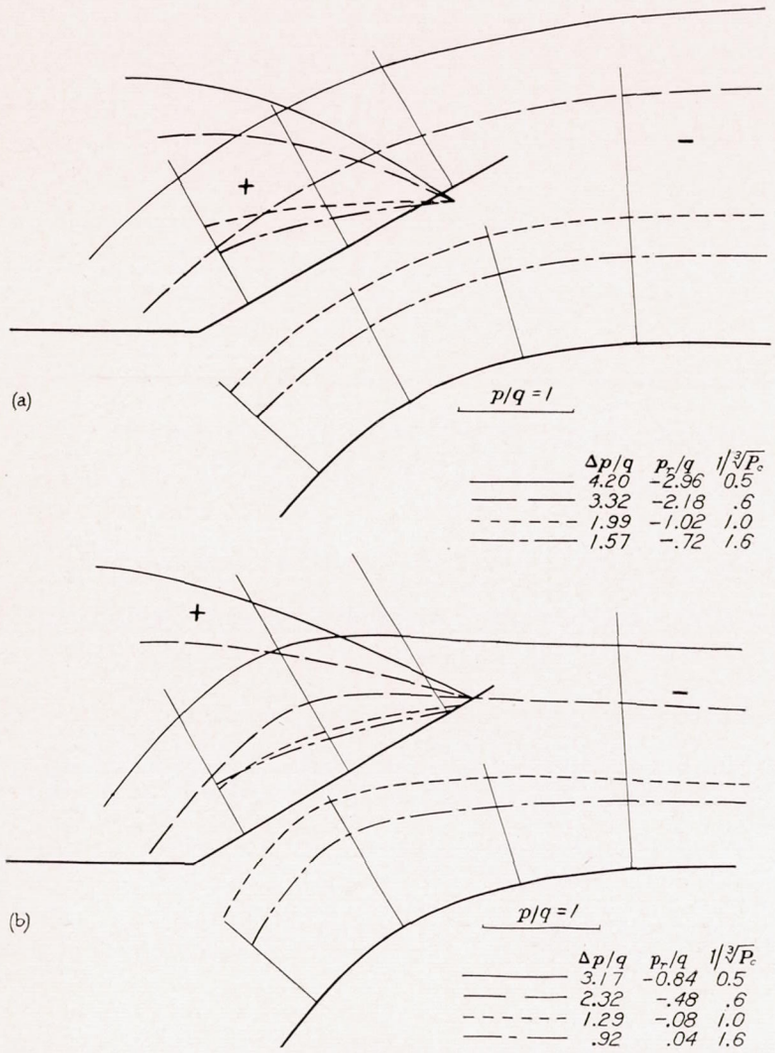

(a) $K=0$.
(b) $K=0.118$.

FIGURE 6.—Pressure distribution for the 30° flap. Propeller C.

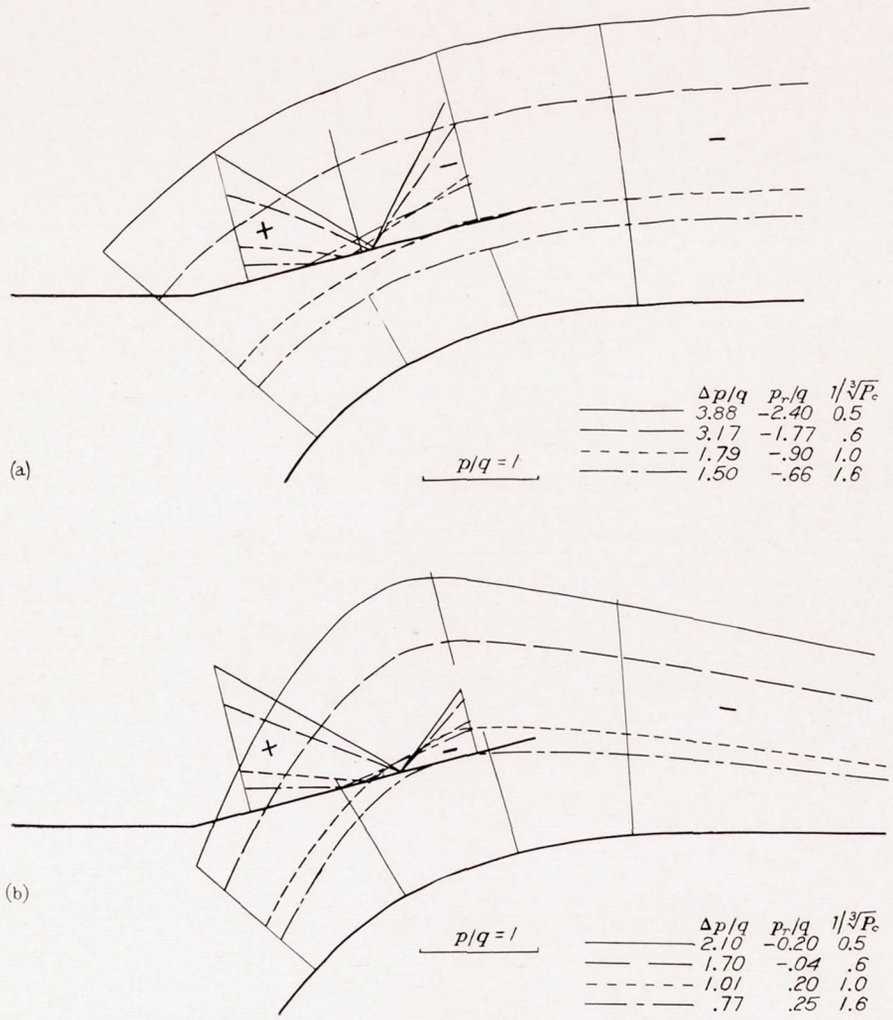

(a) $K=0$.
(b) $K=0.118$.

FIGURE 5.—Pressure distribution for the 15° flap. Propeller C.

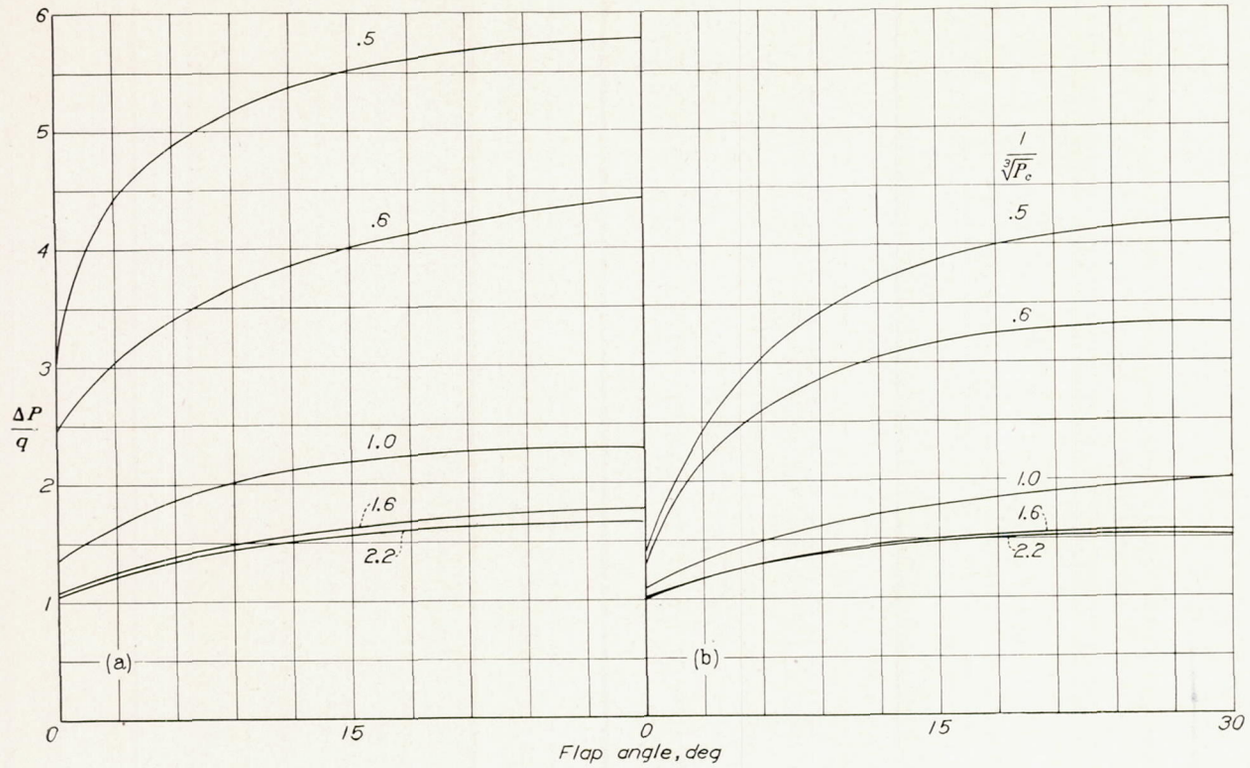

(a) Propeller F. (b) Propeller C.

FIGURE 7.—Available pressure difference.

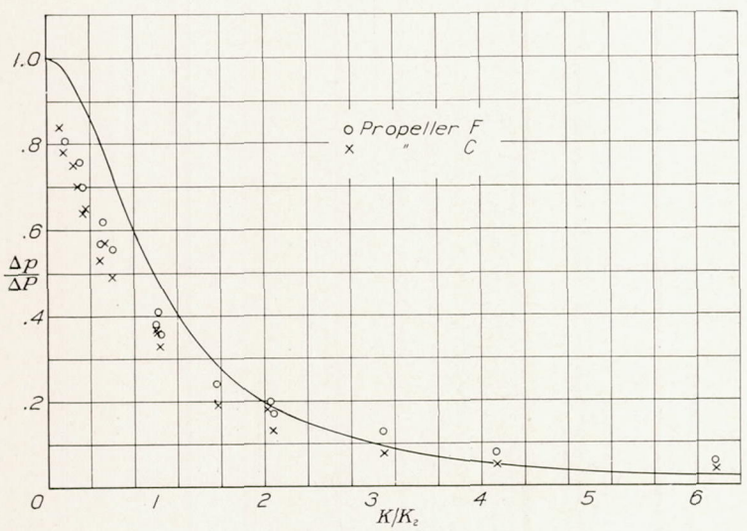

FIGURE 8.—Graphical solution of the flow equation. The 0° flap at the high-speed condition, $1/\sqrt[3]{P_c}=1.6$.

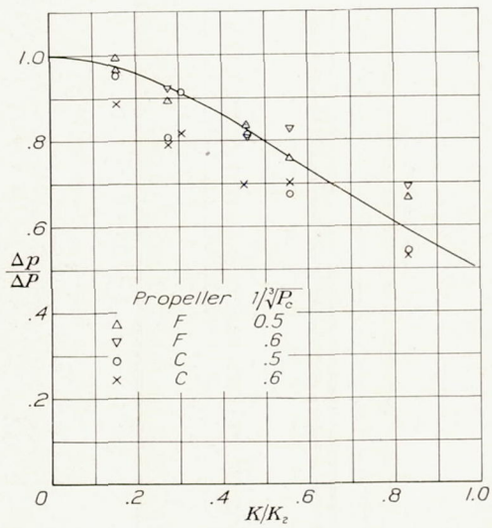

FIGURE 9.—Graphical solution of the flow equation. The 15° and the 30° flaps at the take-off condition.

For $1/\sqrt[3]{P_c}=0.5$, propeller C is 47 percent efficient, giving an average increase in total pressure in the slipstream of 3.76 times the dynamic pressure in the main air stream. (The average values of $H/q=T_c$ corresponding to the given values of $1/\sqrt[3]{P_c}$ may be obtained from reference 5.) Reference to table I for the operating condition of $1/\sqrt[3]{P_c}=0.5$ and $K=0$ shows that the average front pressure obtained for propeller C is 1.25 times the dynamic pressure of the main air stream, an increase in total pressure of $0.25q$ over the dynamic pressure of the air stream. The average increase in total pressure in the slipstream being $3.76q$, only one-fifteenth of this average pressure increase is seen to be available for front pressure on the test set-up.

The average front pressure obtained for propeller F under conditions similar to those for propeller C is $2.67q$, or an increase in total pressure of $1.67q$ over the dynamic pressure of the air stream. When air is flowing through the cowling, the front pressure becomes still greater. For the condition of $1/\sqrt[3]{P_c}=0.5$, the pressure added by propeller C increased from $0.25q$

for zero air flow to $1.33q$ for a conductance of 0.118 with the 30° flap; under the same conditions, the pressure added by propeller F increased from $1.67q$ to $2.93q$. This large change in front pressure with air flow at low speed is largely an effect of the change in the effective diameter of the opening as a result of changing the streamlines in front of the cowling. If the cowling opening were not located in such a critical pressure region, the change in pressure with air flow would be nearly negligible. For the high-speed condition, $1/\sqrt[3]{P_c}=1.6$, the pressure remains approximately constant with radius.

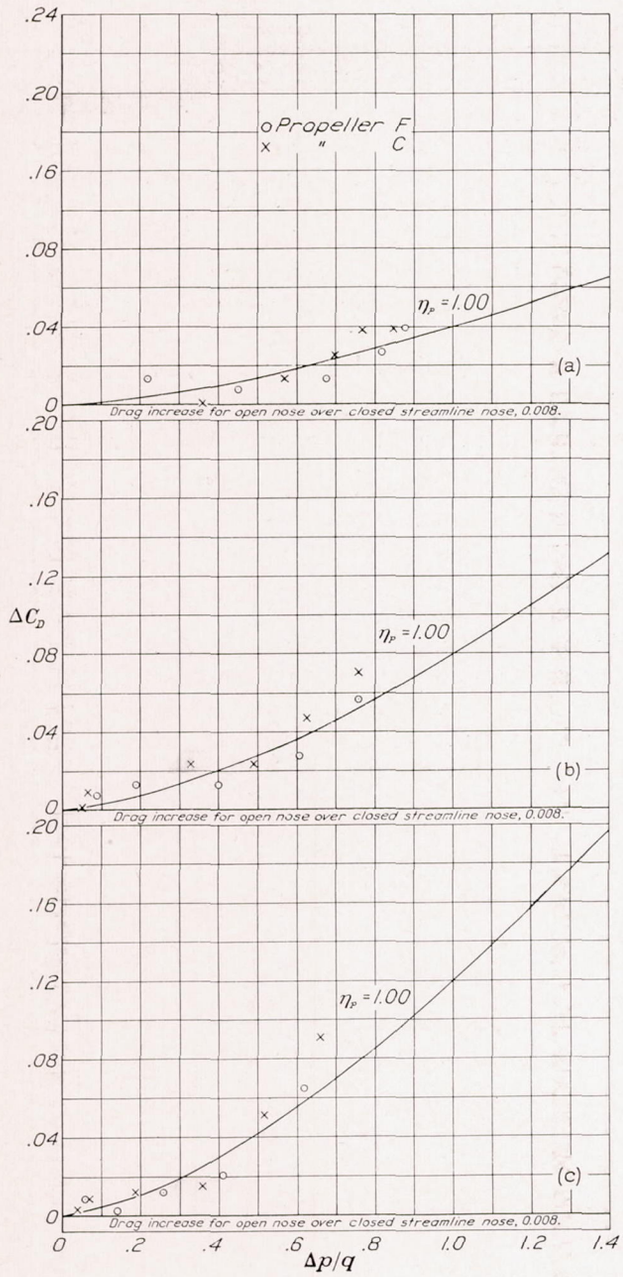

(a) K=0.039. (b) K=0.079. (c) K=0.118.

FIGURE 10.—Variation of cooling-drag coefficient with pressure drop at $1/\sqrt[3]{P_c}=1.6$.

The effect of larger propellers, say 17 feet in diameter, on this same 52-inch nacelle is interesting. Propeller diameters of 10 and 17 feet on this nacelle represent the maximum and the minimum ratios of F/S encountered in present-day design. With the 17-foot propeller the maximum diameter of the front opening will have a value of x of 0.17 as compared with 0.29 for the 10-foot propeller. It should be realized that, although the available front pressure rapidly decreases for either propeller with a decrease in size of the front opening, the pressure decrease occurs at a smaller value of x with propeller F than with propeller C because of the better blade sections. Although on the test set-up propeller F produced much higher front pressure than propeller C, this large difference in the increase in front pressure would not exist for geometrically similar propellers 17 feet in diameter on the test nacelle. Both propellers would probably give some blocking effect for such an arrangement.

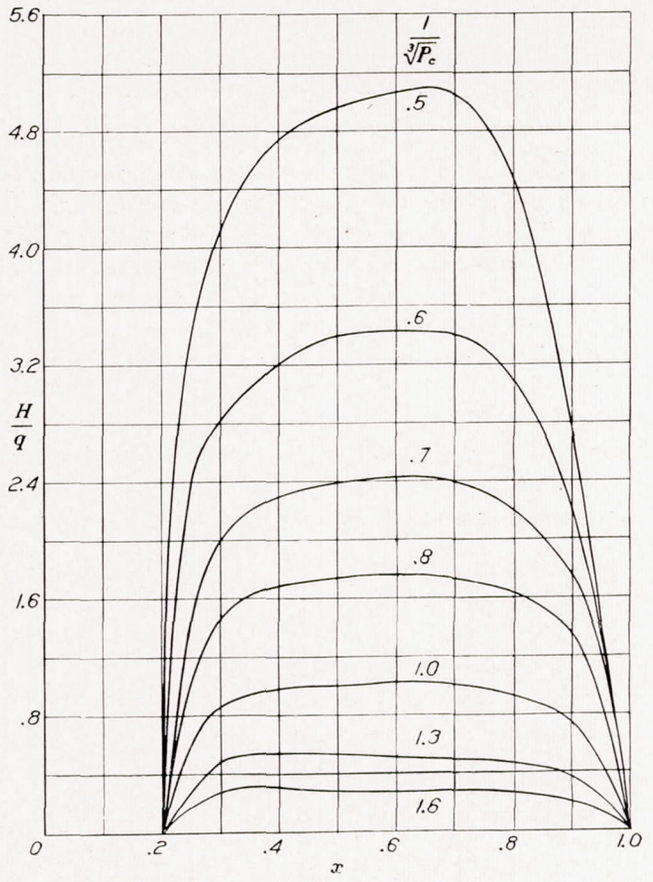

FIGURE 11.—Distribution of pressure increase. Propeller C; β, 20°.

A point of further interest is the front pressure available for ground operation. The manner in which the available front pressure varies with the propeller radius for ground operation is shown in figure 4 of reference 6. For a front opening of $x=0.29$, corresponding to the test arrangement, the available front-pressure coefficient $\frac{p_f \times 10^3}{n^2 D^2}$ is equal to 0.25 for a blade-angle

setting of 20° for propeller C. For a value of $x=0.17$, corresponding to the larger propeller, the front pressure coefficient is only 0.01. In other words, the 17-foot propeller would give essentially zero front pressure for ground cooling. This result illustrates the desirability of airfoil sections on the inner portion of the propeller.

EFFECT OF EXIT SLOT ON THE AVAILABLE PRESSURE

Two effects result from changing the area of the exit slot of a smooth-contour exit design by means of flaps: (1) The increase in the cowling-exit area increases the conductance of the exit slot and, consequently, the pressure drop across the engine; (2) the change in the contour of the cowling in the region of the exit changes the pressure distribution over the cowling and thereby affects the over-all available pressure. These two effects are separately illustrated by the test results and will be separately discussed.

EFFECT OF CHANGING THE EXIT CONDUCTANCE

The effect of changing the exit conductance is illustrated by the tests on the 0° flap for various exit-slot areas. Table I shows the ratio of the pressure behind the baffle plate to the dynamic pressure of the air stream p_r/q to be nearly constant for all conditions of the 0° flap at $K=0$, regardless of the slot opening or the propeller operating condition. An examination of the pressure distribution for the 0° flap with ½-inch exit slot (fig. 4) shows the same result for several conditions of propeller operation. For $K=0$, the static pressure at the slot was nearly zero for all conditions of propeller operation, indicating that the total pressure added by the propeller has been almost entirely converted into dynamic pressure in this region. Any change in the cooling-pressure drop for the 0° flap may therefore be attributed almost entirely to a change in exit conductance. A small secondary change occurs that is due to the change in front pressure.

The solution of the flow equation (equation (1)) given in figure 8 shows that, for large values of K/K_2 (corresponding to small exit openings), the agreement of the points and the theoretical curve is very good; but, for small values of K/K_2, the experimental points fall below the curve. The discrepancy is largely due to the fact that $A_2/F=K_2$ is not a good measure of the conductance for large exit openings.

It may be repeated that the use of $A_2/F=K_2$ in the flow equation will give a first approximation of the change in cooling pressure drop with exit conductance. If the test set-up is reproduced, a closer approximation may be obtained by fairing a curve through the experimental points.

EFFECTS OF CHANGING THE COWLING CONTOUR AT THE EXIT SLOT

The effect of changing the cowling contour at the exit slot is illustrated by the tests of the 15° and the 30° flaps. Table I, $K=0$, shows that p_r/q undergoes a great change when the flap is extended into the slipstream. This change in p_r/q is evidently a result of the deflection of the slipstream, which gives an increase in the local velocity over the exit. This increase in local velocity produces a negative pressure behind the flap. The magnitude of p_r/q is a function of the propeller loading, as is clearly shown by the

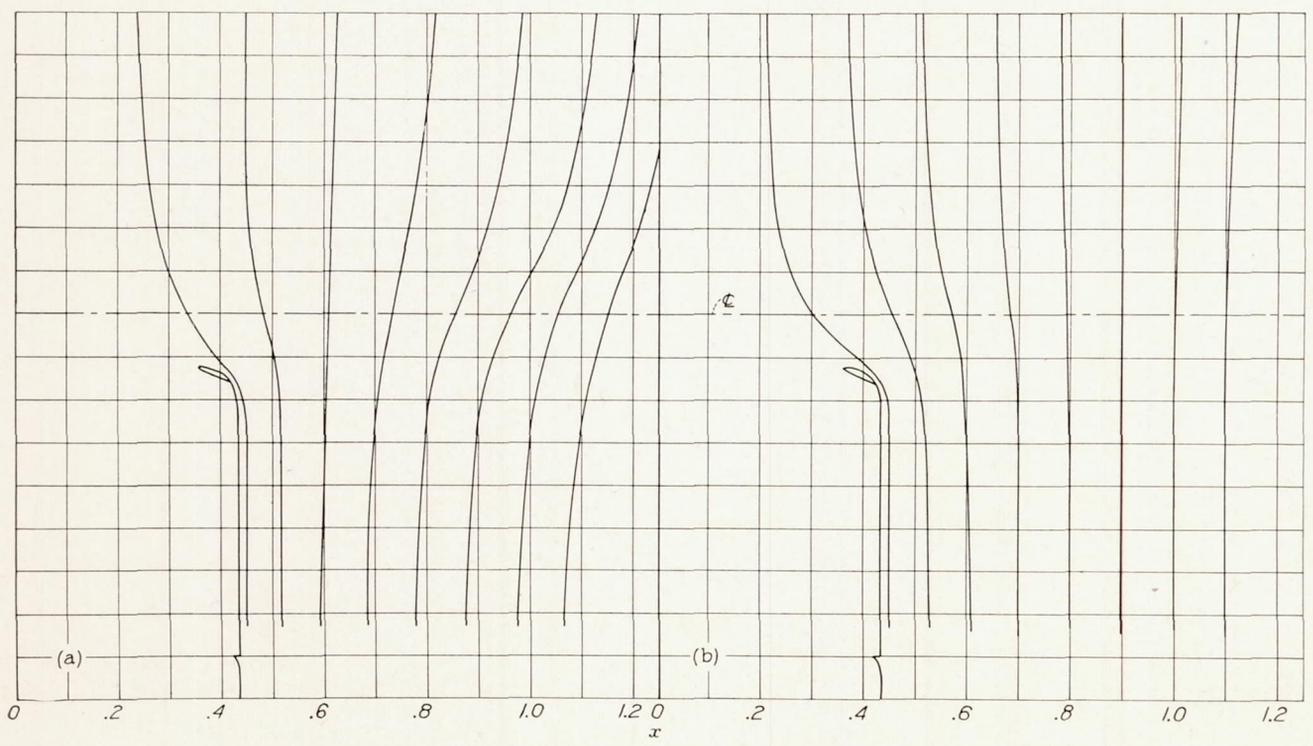

(a) Take-off condition. (b) High-speed condition.

FIGURE 12.—Streamlines around front of cowling. Propeller C.

pressure distributions of figures 5 and 6. The decrease in static pressure for $K=0$ and $1/\sqrt[3]{P_c}=0.5$ behind propeller C is $2.25q$ for the 15° flap and $2.75q$ for the 30° flap; that is, the 15° flap produced a negative pressure of 47 percent and the 30° flap produced a negative pressure of 58 percent of the average dynamic pressure in the slipstream, $4.76q$.

Examination of all the results for zero conductance shows that approximately 55 percent of the average total pressure in the slipstream is available as decreased pressure at the exit slot with the 30° flap. Other unpublished measurements also show that approximately the same decrease in static pressure may be obtained for the static condition, where the average dynamic pressure in the slipstream is given by T/S.

Table I shows that the values of the negative pressures for propeller F are somewhat larger than those for propeller C. This increase in negative pressure for propeller F is due to a change in the distribution of the total-pressure increase behind the propeller, which concentrates more of the thrust over the inner sections of the propeller.

The effect of air flow through the slot for both the 15° and the 30° flaps is shown in figure 9. Although the scatter of the test points is explained by the inability accurately to determine K_2, the points above the theoretical curve are due in part to the increase in front pressure with air flow.

No data are available concerning the effect on the pressure at the exit obtained by varying the propeller diameter with respect to the nacelle diameter, but it is believed that a study of the test results will give a good indication of what pressures might be expected with other ratios of propeller to nacelle diameter. For example, consider the 17-foot geometrically similar propeller on the same nacelle. The exit slot in this case is located at a value of x of 0.255. Inasmuch as the flap produces a pressure drop equivalent to 55 percent of the dynamic pressure in the slipstream for the case tested, it may be estimated that only 45 percent of the $4.76q$, or $2.1q$, should be available as suction at the exit with the 30° flap. Inasmuch as the exit slot would be located in such a critical pressure region for this test combination, opening the flaps might result in a further increase in available pressure for cooling.

EFFICIENCY OF THE EXIT SLOT

For the high-speed flight condition, with a properly designed exit slot, the drag increase caused by the passage of the cooling air is approximately that associated with 100-percent pumping efficiency (fig. 10). The exit must fair smoothly into the nacelle and the air leaving the exit slot must be in the same direction and of approximately the same velocity as that in the outside air stream. If the air from the exit is not in the same direction as that in the air stream, it will cause an upset of the main air flow with a resultant drag increase. Very low efficiencies usually indicate improper exit conditions. The low efficiencies shown in table I associated with the small exits, such as the ¼-inch slot, do not necessarily indicate poor exit-slot designs but are probably due to inaccuracies in measurements.

For the low-speed-flight condition, the pumping efficiency is of secondary importance; the primary requisite is large available pressure for cooling. It has already been shown that the extended flap is a very effective means of producing large available pressure differences.

The extended flap causes a break in the air flow, which in turn causes the pumping efficiency to fall below 100 percent. For the take-off condition, the difference in net efficiency is too small to permit the pump efficiency to be accurately computed. The pumping efficiencies are included for the 15° and the 30° flaps at $1/\sqrt[3]{P_c}=1.0$, corresponding to the climb condition. For $K=0.118$, the value of η_p falls from 0.76 for the 15° flap to 0.39 for the 30° flap for propeller F and from 0.59 for the 15° flap to 0.32 for the 30° flap for propeller C. Part of this large decrease in η_p for the 30° flap is, of course, due to the disturbance of the air flow, but a part of it is due to the fact that the 30° flap does not contract the cooling air all the way to the exit. This condition may be seen in figure 6, where the maximum velocity, that is, the lowest pressure, is observed forward of the exit.

DESIGN COMPUTATIONS

It has been shown how the pressure available for cooling with cowling flaps is dependent on the conditions in the propeller slipstream; that is, how the total, the static, and the velocity pressures vary with the propeller operating condition. In order to illustrate the application of these results, two typical design computations are given. Case 1 simulates the test set-up and case 2 applies the results to a different ratio of cowling diameter to propeller diameter corresponding to a more modern design of engine-propeller installation.

The specifications for the two cases are given in table II.

The cowling specifications must now be determined for the various conditions of operation. The diameter is taken as 52 inches for case 1 and as 60 inches for case 2. The estimates for both cases are for propellers similar to propeller C. A propeller with better airfoil sections on the inner portion will produce greater pressure differences.

TABLE II

DATA FOR DESIGN COMPUTATIONS

	Case 1	Case 2
Engine:		
Power output, hp	550	2,000
Indicated power, hp	650	2,300
Altitude rating, ft	0–10,000	0–15,000
Take-off power, hp	650	2,300
Δp required for cooling at rated power and altitude, lb/sq ft	25	40
Indicated power at one-half rated speed and minimum blade-angle setting, hp	100	310
Δp required for cooling at one-half rated speed and minimum blade-angle setting, lb/sq ft	1.0	1.2
Maximum engine diameter, in.	52	60
Engine-baffle conductance, K	.06	.15
Airplane:		
Top speed at rated altitude, mph	230	300
Dynamic pressure at top speed and rated altitude, lb/sq ft	100	145
Cruising speed, mph	209	270
Best climbing speed, mph	110	145
Dynamic pressure for climbing speed at sea level, lb/sq ft	31	54
Propeller:		
Type of control	(1)	(1)
Number of blades	3	3
Speed at rated engine speed, rpm	1,500	900
Diameter, ft	10	17
Blade-angle setting at top speed and rated altitude, deg	32½	38½
Blade-angle setting for full-power climb at best climbing speed, deg	22	25
Minimum blade-angle setting, deg	15	16
Power asborbed at one-half rated speed and minimum blade-angle setting, hp	50	160

[1] Constant speed.

Top speed.—The computation for the top-speed condition is quite straightforward.

	Case 1	Case 2
ΔP(for $\Delta P/q=1$), lb/sq ft	100	145
$\Delta P/\Delta p$	4.00	3.63
$K/K_2=\sqrt{\Delta P/\Delta p-1}$	1.73	1.62
$K_2=A_2/F$	0.0346	0.0925
Width of exit slot (¼ diam.$\times A_2/F$), in.	½	1⅜

Full-power climb.—For the full-power climb, $\Delta P/q$ must first be known. For case 1, this value is easily obtained from figure 7 (b). For case 2, the estimate may be made in the following manner:

In a climb at 145 miles per hour with 2000 horsepower being absorbed by a 17-foot propeller, $1/\sqrt[3]{P_c}=1.33$, or $P_c=0.425$. With an efficiency of 80 percent, $T_c=0.34$; that is, the increase in total pressure behind the propeller is $0.34q$. For this combination, 45 percent of the total pressure of the slipstream may be developed by the 30° flap; 45 percent of 1.34 is 0.60. Now, because of the large propeller hub, an allowance must be made for blocking, and a front pressure of only $0.7q$ may be assumed. The over-all available pressure difference is thus $1.3q$.

	Case 1	Case 2
$1/\sqrt[3]{P_c}$	1.09	1.33
$\Delta P/q$	1.7	1.3
ΔP, lb/sq ft	53	70
$\Delta P/\Delta p$	2.11	1.75
K/K_2	1.05	0.87
K_2	0.057	0.173
Width of exit slot, in.	¾	2⅝

Take-off.—Probably the condition of greatest interest is the take-off or immediately thereafter. Computations similar to the preceding ones indicate that, for case 1, satisfactory cooling is obtained with a 2⅝-inch flap opening at $1/\sqrt[3]{P_c}=0.5$ at an airspeed of 50 miles per hour. The conditions for case 2 are more severe, a 5⅝-inch opening being required for $1/\sqrt[3]{P_c}=1.0$ at 109 miles per hour. For this case, an efficiency of 72 percent and, because of the greater thrust coefficient, a front pressure of $0.8q$ were assumed.

	Case 1	Case 2
$1/\sqrt[3]{P_c}$	0.5	1.0
$\Delta P/q$	4.20	1.57
ΔP, lb/sq ft	27.3	46.3
$\Delta P/\Delta p$	1.09	1.16
K/K_2	0.30	0.40
K_2	0.20	0.375
Width of exit slot, in.	2⅝	5⅝

Ground operation.—The cooling estimate for ground operation is made for the static-thrust condition at one-half engine speed and minimum blade-angle setting. A conservative estimate will be made by assuming the front pressure to be zero. If the flap setting is the same as for the take-off condition, $\Delta P/\Delta p$ will also be the same.

	Case 1	Case 2
C_T (static)	0.13	0.135
$H=T/S$, lb/sq ft	6.15	6.64
$\Delta P=-p_r$, lb/sq ft	3.38	2.99
$\Delta P/\Delta p$	1.09	1.16
Δp produced, lb/sq ft	3.1	2.6
Δp required, lb/sq ft	1.0	1.2

Thus, the engine should be adequately cooled under ordinary ground operating conditions.

CONCLUSIONS

1. The pressure available for cooling is shown to be a direct function of the thrust disk-loading coefficient of the propeller.

2. The maximum suction obtained with a 30° cowling flap located in a region where the static pressure for the 0° flap is equal to that of the free air stream is shown to be equal to approximately one-half the average total pressure of the propeller slipstream, which is given by the sum of the dynamic pressure and the thrust loading.

3. The total pressure in front of the cowling is critically dependent on the ratio of the front opening to the propeller diameter for round-shank propeller C. Propeller F, with airfoil sections closer to the hub, gave a higher total pressure in front of the cowling.

4. For the take-off condition with the 0° flap, propeller C produced only one-half as much available cooling pressure as propeller F.

5. For this same operating condition with the 30° flap, propeller C produced an available cooling pressure three times as large as was obtained with the 0° flap and propeller F produced a pressure difference twice that obtained with the 0° flap.

6. For the take-off condition, the 30° flap, and a conductance of 0.118, the pressure drop across the the baffle plate with propeller C was 3.17 and with propeller F was 4.85 times the dynamic pressure of the air stream.

LANGLEY MEMORIAL AERONAUTICAL LABORATORY,
NATIONAL ADVISORY COMMITTEE FOR AERONAUTICS,
LANGLEY FIELD, VA., *May 9, 1940.*

REFERENCES

1. Theodorsen, Theodore, Brevoort, M. J., and Stickle, George W.: Full-Scale Tests of N.A.C.A. Cowlings. Rep. No. 592, NACA, 1937.
2. Theodorsen, Theodore, Brevoort, M. J., and Stickle, George W.: Cooling of Airplane Engines at Low Air Speeds. Rep. No. 593, NACA, 1937.
3. Theodorsen, Theodore, Brevoort, M. J., Stickle, George W., and Gough, M. N.: Full-Scale Tests of a New Type N.A.C.A. Nose-Slot Cowling. Rep. No. 595, NACA, 1937.
4. Weick, Fred. E., and Wood, Donald H.: The Twenty-Foot Propeller Research Tunnel of the National Advisory Committee for Aeronautics. Rep. No. 300, NACA, 1928.
5. Stickle, George W., Crigler, John L., and Naiman, Irven: Effect of Body Nose Shape on the Propulsive Efficiency of a Propeller. Rep. No. 725, NACA, 1941.
6. Stickle, George W., and Joyner, Upshur T.: The Pressure Available for Ground Cooling in Front of the Cowling of Air-Cooled Airplane Engines. T. N. No. 673, NACA, 1938.

TABLE I– CONDENSED EXPERIMENTAL RESULTS

Flap angle (deg)	Slot opening (in.)	Propeller	$\frac{A_2}{F}$	$1/\sqrt[3]{P_c}=0.5$			$1/\sqrt[3]{P_c}=0.6$			$1/\sqrt[3]{P_c}=1.0$				$1/\sqrt[3]{P_c}=1.6$				C_D
				$\frac{\Delta p}{q}$	$\frac{p_r}{q}$	η_n	$\frac{\Delta p}{q}$	$\frac{p_r}{q}$	η_n	$\frac{\Delta p}{q}$	$\frac{p_r}{q}$	η_n	η_p	$\frac{\Delta p}{q}$	$\frac{p_r}{q}$	η_n	η_p	Estimated
CONDUCTANCE=0																		
0	0.00	F				0.488			0.552			0.716				0.753		0.081
0	.25	F	0.019	2.82	−0.27	.482	2.23	−0.22	.549	1.34	−0.15	.714		1.09	−0.14	.753		.084
0	.50	F	.038	3.05	−.22	.488	2.78	−.18	.550	1.37	−.16	.716		1.10	−.16	.754		.085
0	1.00	F	.075	2.80	−.26	.485	2.39	−.25	.548	1.40	−.16	.714		1.10	−.16	.753		.085
0	1.75	F	.131	2.79	−.12	.492	2.46	−.12	.556	1.38	−.14	.713		1.08	−.16	.750		.086
0	3.25	F	.238	2.76	−.02	.482	2.43	−.07	.544	1.31	−.12	.719		1.08	−.14	.751		.087
15	1.75	F	.142	5.52	−2.54	.474	4.01	−1.89	.540	2.20	−.97	.687		1.64	−.70	.686		.165
30	3.25	F	.259	5.78	−3.15	.462	4.42	−2.29	.521	2.30	−1.12	.654		1.77	−.82	.541		.326
0	.00	C				.472			.542			.721				.770		
0	.25	C	.019	1.24	−.28	.478	1.30	−.24	.549	1.14	−.15	.723		1.00	−.15	.773		
0	.50	C	.038	1.52	−.16	.472	1.43	−.16	.543	1.09	−.15	.712		.99	−.15	.771		
0	1.00	C	.075	1.52	−.13	.482	1.44	−.14	.550	1.11	−.15	.714		1.00	−.16	.773		
0	1.75	C	.131	1.37	−.20	.474	1.29	−.15	.539	1.10	−.14	.713		1.00	−.16	.767		
0	3.25	C	.238	1.07	−.02	.473	1.17	−.05	.539	1.06	−.11	.721		.99	−.14	.768		
0	4.62	C	.336	1.37	−.09	.473	1.38	−.10	.540	1.07	−.14	.721		1.01	−.17	.762		.095
15	1.75	C	.142	3.88	−2.40	.472	3.17	−1.77	.538	1.79	−.90	.700		1.50	−.66	.706		
30	3.25	C	.259	4.20	−2.96	.454	3.32	−2.18	.518	1.99	−1.02	.658		1.57	−.72	.571		
CONDUCTANCE=0.039																		
0	0.00	F				0.488			0.552			0.716				0.753		
0	.25	F	0.019	1.44	1.64	.483	1.17	1.30	.552	0.47	0.79	.716		0.22	0.70	.744	0.31	0.090
0	.50	F	.038	1.88	1.20	.486	1.47	.99	.548	.70	.59	.716		.45	.53	.748	1.50	.094
0	1.00	F	.075	2.14	.73	.485	1.62	.58	.548	.86	.34	.713		.68	.29	.744	1.67	.108
0	1.75	F	.131	2.24	.58	.488	1.86	.44	.558	1.07	.21	.718		.82	.16	.734	1.11	.116
0	3.25	F	.238	2.40	.43	.483	1.97	.33	.547	1.14	.13	.708		.88	.09	.724	.82	.124
15	1.75	F	.142	4.94	−1.64	.478	3.69	−1.21	.539	1.85	−.59	.681	0.52	1.42	−.40	.638	.44	.222
30	3.25	F	.259	5.73	−2.38	.459	4.28	−1.73	.514	2.12	−.75	.632	.27	1.58	−.57	.472	.21	.422
0	.00	C				.472			.542			.721				.770		
0	.25	C	.019	.38	.90	.479	.38	.80	.549	.25	.68	.725		.18	.68	.774	∞	
0	.75	C	.038	.64	.70	.472	.55	.65	.542	.40	.53	.716		.36	.51	.770	∞	
0	1.00	C	.075	.84	.47	.480	.86	.41	.548	.71	.30	.716		.57	.27	.760	1.28	
0	1.75	C	.131	1.00	.36	.476	.95	.30	.545	.78	.19	.713		.70	.17	.751	.92	
0	3.25	C	.238	.92	.35	.476	.98	.26	.542	.86	.13	.711		.77	.11	.741	.70	
0	4.62	C	.336	1.39	.15	.472	1.26	.12	.545	.95	.05	.712		.85	.02	.740	.78	.132
15	1.75	C	.142	3.14	−1.66	.472	2.52	−1.23	.536	1.50	−.48	.686	.39	1.27	−.32	.660	.39	
30	3.25	C	.259	3.70	−2.13	.453	2.94	−1.54	.514	1.65	−.66	.640	.19	1.28	−.39	.481	.15	
CONDUCTANCE=0.079																		
0	0.00	F				0.488			0.552			0.716				0.753		
0	.25	F	0.019	0.75	1.91	.483	0.60	1.57	.551	0.25	0.97	.709		0.09	0.84	.748	0.86	0.090
0	.50	F	.038	1.13	1.74	.492	.84	1.36	.553	.34	.86	.717		.19	.77	.753	5.14	.093
0	1.00	F	.075	1.57	1.33	.484	1.12	1.05	.549	.57	.69	.713		.40	.60	.744	1.53	.103
0	1.75	F	.131	1.66	1.10	.488	1.38	.86	.551	.74	.52	.714		.61	.43	.733	1.37	.120
0	3.25	F	.238	1.93	.88	.486	1.53	.70	.546	1.00	.40	.710		.76	.31	.711	.93	.135
15	1.75	F	.142	4.18	−.79	.477	3.32	−.56	.538	1.62	−.18	.676	0.76	1.19	−.08	.618	.58	.247
30	3.25	F	.259	5.25	−1.67	.456	4.05	−1.16	.512	1.86	−.44	.610	.35	1.38	−.27	.412	.29	.500
0	.00	C				.472			.542			.721				.770		
0	.25	C	.019	.18	1.13	.478	.17	1.00	.549	.11	.85	.720		.05	.78	.769	.68	
0	.50	C	.138	.42	1.00	.477	.34	.89	.545	.19	.75	.713		.13	.73	.763	.62	
0	1.00	C	.175	.50	.83	.477	.47	.76	.548	.38	.62	.716		.33	.57	.752	.64	
0	1.75	C	.131	.71	.73	.475	.70	.65	.543	.53	.47	.708		.49	.43	.752	1.15	
0	3.25	C	.238	.71	.65	.477	.73	.55	.540	.70	.35	.713		.63	.30	.734	.84	
0	4.62	C	.336	1.07	.48	.476	1.02	.37	.549	.82	.23	.711		.76	.20	.716	.74	.165
15	1.75	C	.142	2.63	−.88	.472	2.22	−.60	.533	1.23	−.17	.678	.47	.98	−.03	.634	.42	
30	3.25	C	.259	3.55	−1.44	.452	2.72	−.96	.512	1.46	−.34	.620	.26	1.14	−.15	.414	.21	
CONDUCTANCE=0.118																		
0	0.00	F				0.488			0.552			0.716				0.753		
0	.25	F	0.019	0.33	2.21	.474	0.33	1.75	.551	0.18	1.04	.713		0.06	0.89	.748	0.22	0.089
0	.50	F	.038	.54	2.03	.484	.50	1.59	.549	.23	.95	.719		.14	.86	.752	2.37	.093
0	1.00	F	.075	.86	1.78	.486	.76	1.36	.552	.42	.87	.714		.26	.76	.743	1.08	.097
0	1.75	F	.131	1.30	1.48	.478	1.13	1.16	.543	.64	.72	.710		.41	.63	.738	1.48	.111
0	3.25	F	.238	1.52	1.26	.478	1.36	.97	.539	.82	.59	.708		.62	.50	.704	.89	.141
15	1.75	F	.142	3.68	.02	.477	2.77	.09	.538	1.30	.16	.673	0.76	.97	.23	.632	.71	.228
30	3.25	F	.259	4.85	−.92	.456	3.58	−.65	.510	1.67	−.17	.593	.39	1.18	.01	.383	.31	.540
0	.00	C				.472			.542			.721				.770		
0	.25	C	.019	.13	1.22	.479	.12	1.05	.549	.05	.87	.719		.04	.80	.768	.36	
0	.50	C	.138	.14	1.16	.480	.14	1.04	.547	.10	.83	.713		.07	.78	.764	.28	
0	1.00	C	.175	.46	1.06	.482	.40	.93	.549	.24	.75	.717		.19	.70	.761	.84	
0	1.75	C	.131	.36	.97	.478	.39	.84	.542	.38	.64	.714		.36	.60	.758	1.63	
0	3.25	C	.238	.73	.81	.480	.72	.75	.542	.57	.53	.709		.52	.48	.731	.87	
0	4.62	C	.336	.89	.74	.478	.89	.62	.546	.73	.42	.709		.66	.35	.700	.69	.179
15	1.75	C	.142	2.10	−.20	.472	1.70	−.04	.538	1.01	.20	.683	.59	.77	.25	.642	.48	
30	3.25	C	.259	3.17	−.84	.448	2.32	−.48	.503	1.29	−.08	.620	.32	.92	.04	.384	.21	

U. S. GOVERNMENT PRINTING OFFICE: 1941

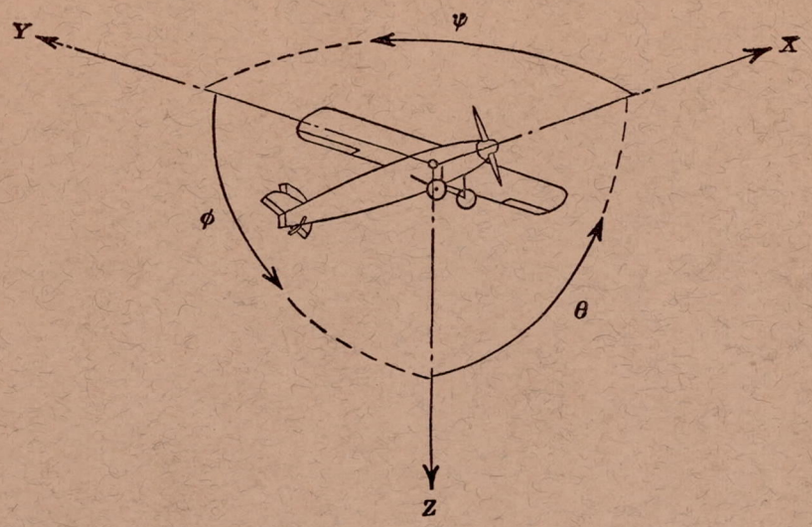

Positive directions of axes and angles (forces and moments) are shown by arrows

Axis		Force (parallel to axis) symbol	Moment about axis			Angle		Velocities	
Designation	Symbol		Designation	Symbol	Positive direction	Designation	Symbol	Linear (component along axis)	Angular
Longitudinal	X	X	Rolling	L	$Y \longrightarrow Z$	Roll	ϕ	u	p
Lateral	Y	Y	Pitching	M	$Z \longrightarrow X$	Pitch	θ	v	q
Normal	Z	Z	Yawing	N	$X \longrightarrow Y$	Yaw	ψ	w	r

Absolute coefficients of moment

$C_l = \frac{L}{qbS}$ (rolling) $\quad C_m = \frac{M}{qcS}$ (pitching) $\quad C_n = \frac{N}{qbS}$ (yawing)

Angle of set of control surface (relative to neutral position), δ. (Indicate surface by proper subscript.)

4. PROPELLER SYMBOLS

D, Diameter

p, Geometric pitch

p/D, Pitch ratio

V', Inflow velocity

V_s, Slipstream velocity

T, Thrust, absolute coefficient $C_T = \frac{T}{\rho n^2 D^4}$

Q, Torque, absolute coefficient $C_Q = \frac{Q}{\rho n^2 D^5}$

P, Power, absolute coefficient $C_P = \frac{P}{\rho n^3 D^5}$

C_s, Speed-power coefficient $= \sqrt[5]{\frac{\rho V^5}{P n^2}}$

η, Efficiency

n, Revolutions per second, r.p.s.

Φ, Effective helix angle $= \tan^{-1}\left(\frac{V}{2\pi r n}\right)$

5. NUMERICAL RELATIONS

1 hp.=76.04 kg-m/s=550 ft-lb./sec.

1 metric horsepower=1.0132 hp.

1 m.p.h.=0.4470 m.p.s.

1 m.p.s.=2.2369 m.p.h.

1 lb.=0.4536 kg.

1 kg=2.2046 lb.

1 mi.=1,609.35 m=5,280 ft.

1 m=3.2808 ft.